

Observer-based dynamic event-triggered control for distributed parameter systems over mobile sensor-plus-actuator networks

Wenying Mu(穆文英), Bo Zhuang(庄波), and Fang Qiu(邱芳)

Citation: Chin. Phys. B, 2024, 33 (**4**): 040204. DOI: 10.1088/1674-1056/ad1a8c
Journal homepage: http://cpb.iphy.ac.cn; http://iopscience.iop.org/cpb

What follows is a list of articles you may be interested in

Quintessence anisotropic stellar models in quadratic and Born-Infeld modified teleparallel Rastall gravity

Allah Ditta, Tiecheng Xia(夏铁成), Irfan Mahmood, and Asif Mahmood
Chin. Phys. B, 2024, 33 (**3**): 030204. DOI: 10.1088/1674-1056/acfaf9

Discontinuous event-trigger scheme for global stabilization of state-dependent switching neural networks with communication delay

Yingjie Fan(樊英杰), Zhen Wang(王震), Jianwei Xia(夏建伟), and Hao Shen(沈浩)
Chin. Phys. B, 2021, 30 (**3**): 030202. DOI: 10.1088/1674-1056/abc541

Improved control for distributed parameter systems with time-dependent spatial domains utilizing mobile sensor—actuator networks

Jian-Zhong Zhang(张建中), Bao-Tong Cui(崔宝同), Bo Zhuang(庄波)
Chin. Phys. B, 2017, 26 (**9**): 090201. DOI: 10.1088/1674-1056/26/9/090201

Improved control of distributed parameter systems using wireless sensor and actuator networks: An observer-based method

Zheng-Xian Jiang(江正仙), Bao-Tong Cui(崔宝同), Xu-Yang Lou(楼旭阳), Bo Zhuang(庄波)
Chin. Phys. B, 2017, 26 (**4**): 040201. DOI: 10.1088/1674-1056/26/4/040201

Optimal switching policy for performance enhancement of distributed parameter systems based on event-driven control

Mu Wen-Ying (穆文英), Cui Bao-Tong (崔宝同), Lou Xu-Yang (楼旭阳), Li Wen (李纹)
Chin. Phys. B, 2014, 23 (**7**): 070204. DOI: 10.1088/1674-1056/23/7/070204

Observer-based dynamic event-triggered control for distributed parameter systems over mobile sensor-plus-actuator networks

Wenying Mu(穆文英)[1,†], Bo Zhuang(庄波)[2], and Fang Qiu(邱芳)[3]

[1] *Shandong Engineering Research Center of Aeronautical Materials and Devices, Shangdong University of Aeronautics, Binzhou* 256600, *China*
[2] *School of Information Engineering, Shangdong University of Aeronautics, Binzhou* 256600, *China*
[3] *School of Science, Shangdong University of Aeronautics, Binzhou* 256600, *China*

(Received 13 October 2023; revised manuscript received 12 December 2023; accepted manuscript online 4 January 2024)

We develop a policy of observer-based dynamic event-triggered state feedback control for distributed parameter systems over a mobile sensor-plus-actuator network. It is assumed that the mobile sensing devices that provide spatially averaged state measurements can be used to improve state estimation in the network. For the purpose of decreasing the update frequency of controller and unnecessary sampled data transmission, an efficient dynamic event-triggered control policy is constructed. In an event-triggered system, when an error signal exceeds a specified time-varying threshold, it indicates the occurrence of a typical event. The global asymptotic stability of the event-triggered closed-loop system and the boundedness of the minimum inter-event time can be guaranteed. Based on the linear quadratic optimal regulator, the actuator selects the optimal displacement only when an event occurs. A simulation example is finally used to verify that the effectiveness of such a control strategy can enhance the system performance.

Keywords: distributed parameter systems, event-triggered control, mobile sensors, mobile actuators

PACS: 02.30.Jr, 07.07.Df, 07.05.Dz **DOI:** 10.1088/1674-1056/ad1a8c

1. Introduction

Since a distributed parameter system (DPS) has independent time and space variables, it can describe an actual system exactly and comprehensively. Most natural and industrial production processes are characterized by distributed parameter systems, such as population dynamics, infectious disease model,[1] chemical reactor and thermal process,[2] torsional motion of aircraft,[3] and flexible robot.[4] Therefore, a DPS has a wide application background. Several innovative ideas about the control of DPSs have been developed by El-Farra and Christofides,[5] Iftime,[6] Demetriou,[7] Ji and Cui.[8,9]

Due to the rapid development of microelectronics, mobile sensor-plus-actuator networks have been applied widely in many engineering fields to realize process monitoring and control. In particular, sensor and actuator nodes cooperate with each other to sense and perform events in their surrounding environment. In such networks, mobile sensor nodes can move anywhere for monitoring events so as to improve the network performance significantly. Mobile actuator nodes can move to specific locations in the spatial domain and release control signals to improve on control objectives. The mobile sensor-plus-actuator networks have been extensively deployed in agricultural and industrial fields.[10,11] It is challenging to choose this research topic that estimate and control DPS with mobile sensor and actuator networks. Many control schemes of DPSs with such networks have been proposed. Demetriou[12] proposed an integrated abstract framework utilizing mobile sensor-plus-actuator networks to enhance the state estimation and control of DPSs based on the assumption that mobile sensors and actuators were collocated in the networks. Subsequently, Demetriou[13] extended the previous results and utilized mobile agents to further improve the performance of two-dimensional DPSs based on augmented vehicle dynamics. However, the results are not consistent with practical engineering applications. Jiang *et al.*[14] enhanced the control performance of a DPS based on mobile sensor-plus-actuator networks, and designed a stable strategy for mobile agents. In the new guidance policy, mobile sensor and actuator networks were used to enhance the performance of a DPS for time-dependent spatial domains in Ref. [15]. An iterative learning algorithm was developed for two kinds of DPSs utilizing non-collocated mobile sensors and actuators in Ref. [16]. A state estimation guidance approach designed for a class of DPSs with time-varying delay was proposed in Ref. [17].

To date, an event-triggered control mechanism has attracted widespread attention because of its significant lower cost advantage compared to traditional time-triggered control. In an event-triggered control mechanism, the communication or sampling is only initiated by an event. Hence, several potential event-triggered control strategies were developed.[18–21] A more appropriate event-triggered scheme that could decrease the data transmission in discrete-time switched linear systems was considered in Ref. [18]. The consistency issue of multi-agent systems with a distributed adaptive event-triggered control scheme to realize minimum inter-event time was solved in

[†]Corresponding author. E-mail: weny815@126.com

© 2024 Chinese Physical Society and IOP Publishing Ltd

Ref. [19]. A dynamic event-triggered control mechanism with an estimator over the leader-following network was introduced in Ref. [20]. In Ref. [21], a new dynamic event-triggered controller was developed to achieve network synchronization in piecewise smooth systems.

As mentioned above, the event-triggered control strategies were developed only on lumped parameter systems. The event-triggered control strategy of nonlinear DPSs was seldom reported. In Ref. [22] event-triggered observed-based control was presented for improving the control performance of parabolic DPSs with mobile sensors and actuators. However, the event-triggered condition under consideration was non-dynamic. A distributed event-triggered H_∞ filtering control scheme in a DPS based on stochastic switching topology was introduced in Ref. [23], and then extended to the T–S fuzzy DPS under parameter uncertain and actuator faults in Ref. [9]. In Ref. [24] an event-triggered reliable control approach was implemented to improve the transmission efficiency in nonlinear DPS, and a new H_∞ performance indicator was defined to describe the disturbance rejection level. A novel optimal actuator switching policy was addressed in Ref. [25] with an event-triggered control mechanism for DPSs. Although the event-triggered condition is time-varying, it is independent of the system state.

In light of the aforementioned discussion, we are interested in the dynamic event-triggered control issue for a class of DPSs over a mobile sensor-plus-actuator network. An integrating network composed of mobile sensors and actuators with the capabilities of monitoring and controlling is adopted in the spatial domain. Here, each sensor can move in a small region of the domain to provide spatially averaged state estimation information in DPSs. Furthermore, an event-triggered controller is developed based on sampled state estimation to enhance the closed-loop system performance and to ensure that the minimum inter-event interval is bounded. Once an event occurs, the actuator will change the displacement at the beginning of each time interval according to the event-triggered control mechanism. Compared with traditional time-triggered schemes and event-triggered schemes with constant thresholds, the developed dynamic event-triggered scheme can decrease the update frequency of controller and unnecessary sampled data transmission.

This paper is organized as follows: A few mathematical preliminaries and problem formulation are discussed in Section 2. The guidance policy for each mobile sensor agent using the state feedback observer is presented in Section 3. The design of the dynamic event-triggered control for DPS is proposed in Section 4. The guidance optimal placement algorithm of the mobile actuator agents is developed in Section 5. The simulation of a diffusion process is introduced in Section 6. Finally, Section 7 summarizes the results.

Throughout the paper, the following notations are used. The nonnegative real numbers are denoted by $\mathbb{R}^+$; $\langle\cdot\rangle$ and $\|\cdot\|$ denote the inner product and corresponding norm in Hilbert space, respectively; diag$(\cdot)$ denotes a block diagonal matrix. For $(U,\mathcal{S})$ Hilbert spaces, $\mathcal{L}(U,\mathcal{S})$ indicates the space of bounded linear operator from U into $\mathcal{S}$.

2. Problem formulation

A class of transport processes in one spatial dimension is described by

$$\frac{\partial}{\partial t}s(t,v)=\frac{\partial}{\partial v}(\alpha(v)\frac{\partial}{\partial v}s(t,v))+\sum_{i=1}^{m}b(v,v_i^{\mathrm{a}}(t))u_i(t), \quad (1)$$

subject to the Dirichlet boundary conditions

$$s(t,0)=s(t,h)=0,$$

and the initial condition

$$s(0,v)=s_0(v).$$

The output of the DPS (1) is given as

$$y(t)=\begin{bmatrix}y_1(t)\\ \vdots\\ y_n(t)\end{bmatrix}=\begin{bmatrix}\int_0^h c(v,v_1^{\mathrm{s}}(t))s(t,v)\,\mathrm{d}v\\ \vdots\\ \int_0^h c(v,v_n^{\mathrm{s}}(t))s(t,v)\,\mathrm{d}v\end{bmatrix}, \quad (2)$$

where $s(t,v)$ denotes the system state, $t\in[0,+\infty)$ denotes the time variable; $v\in\Omega=[0,h]\subset\mathbb{R}^+$ denotes the spatial variable; the thermal diffusivity $\alpha(v)\geq\alpha_0>0$; $u_i(t)$ denotes the control input signal; $y(t)$ denotes the system output. The function $b(v,v_i^{\mathrm{a}}(t))$ and spatial point $v_i^{\mathrm{a}}(t)$ denote the i-th mobile actuating device and its time-varying centroid, respectively, where $i=1,\ldots,m$. The function $c(v,v_i^{\mathrm{s}}(t))$ and spatial point $v_i^{\mathrm{s}}(t)\in[0,h]$ denote the i-th mobile sensing device and its time-varying centroid, respectively, where $i=1,\ldots,n$. The time dependence reflects the time variation of the position of sensing and actuating devices in the space domain Ω.

The second-order elliptic operator $\mathcal{A}\in\mathcal{L}(\mathcal{S},\mathcal{S})$ in Hilbert space is defined as

$$\mathcal{A}\phi=\frac{\mathrm{d}}{\mathrm{d}v}(\alpha(v)\frac{\mathrm{d}\phi}{\mathrm{d}v}),\ \ \alpha(v)>0,\ \ \phi\in D(\mathcal{S}),$$

where $D(\mathcal{A})$ is the domain with $D(\mathcal{A})=H_0^1(0,h)\cap H^2(0,h)$. The system (1) can be transformed into a differential equation in Hilbert space $\mathcal{S}$:

$$\dot{s}(t)=\mathcal{A}s(t)+\mathcal{B}(v^{\mathrm{a}}(t))u(t),\ \ s(0)=s_0\in\mathcal{S}, \quad (3)$$

with the system output

$$y(t)=\mathcal{C}(v^{\mathrm{s}}(t))s(t). \quad (4)$$

The input operator $\mathcal{B}\in\mathcal{L}(U,\mathcal{S})$ is given as

$$\langle\mathcal{B}(v^{\mathrm{a}}(t))u(t),\phi\rangle=\int_0^h b(v,v^{\mathrm{a}}(t))\phi(v)u(t)\,\mathrm{d}v,$$

or

$$\mathcal{B}(v_i^{\mathrm{a}}(t))u_i(t) = b(v, v_i^{\mathrm{a}}(t))u_i(t),$$

with the moving actuator locations $v^{\mathrm{a}}(t) = [v_1^{\mathrm{a}}(t), v_2^{\mathrm{a}}(t), \ldots, v_m^{\mathrm{a}}(t)]$, where the function $b(v, v_i^{\mathrm{a}}(t))$ takes the form

$$b(v, v^{\mathrm{a}}(t)) = \begin{cases} 1, & \text{if } v \in [v^{\mathrm{a}}(t) - \xi, v^{\mathrm{a}}(t) + \xi], \\ 0, & \text{otherwise.} \end{cases}$$

It indicates that the actuator device delivers control signals in a spatial area with length 2ξ centered at v^{a}.

The output operator $\mathcal{C} \in \mathcal{L}(\mathcal{S}, Y)$ is defined with the moving sensor location $v^{\mathrm{s}}(t) = [v_1^{\mathrm{s}}(t), v_2^{\mathrm{s}}(t), \ldots, v_n^{\mathrm{a}}(t)]$ via

$$\begin{aligned} \langle \mathcal{C}(v^{\mathrm{s}}(t))\phi, \varphi \rangle &= \begin{bmatrix} \langle \mathcal{C}(v_1^{\mathrm{s}}(t))\phi_1, \phi_2 \rangle \\ \vdots \\ \langle \mathcal{C}(v_n^{\mathrm{s}}(t))\phi_1, \phi_2 \rangle \end{bmatrix} \\ &= \begin{bmatrix} \int_0^h c(v, v_1^{\mathrm{s}}(t))\phi_1(v)\phi_2(v)\,\mathrm{d}v \\ \vdots \\ \int_0^h c(v, v_n^{\mathrm{s}}(t))\phi_1(v)\phi_2(v)\,\mathrm{d}v \end{bmatrix} \end{aligned}$$

for $\phi_1, \phi_2 \in \mathcal{S}$. The function of the sensor spatial distribution is expressed as

$$c(v, v^{\mathrm{s}}(t)) = \begin{cases} 1, & \text{if } v \in [v^{\mathrm{s}}(t) - \varepsilon, v^{\mathrm{s}}(t) + \varepsilon], \\ 0, & \text{otherwise.} \end{cases} \tag{5}$$

3. Guidance of mobile sensor agents

It is assumed that the mobile sensor agents are mainly used to collect data and preprocess measurement information $y(t)$ of DPSs in the covered space domain with the state observer as follows:

$$\dot{\bar{s}}(t) = \mathcal{A}\bar{s}(t) + \mathcal{B}(v^{\mathrm{a}}(t))u(t) + L[y(t) - \mathcal{C}(v^{\mathrm{s}}(t))\bar{s}(t)], \tag{6}$$

where $\bar{s}(t)$ and L are the system state estimate and properly designed observer gain, respectively.

The observation error is defined as

$$\begin{aligned} \dot{\zeta}(t) = \dot{\bar{s}}(t) - \dot{s}(t) &= \mathcal{A} - L\mathcal{C}(v^{\mathrm{s}}(t))\zeta(t) \\ &= \mathcal{A}_{LC}(v^{\mathrm{s}}(t))\zeta(t). \end{aligned} \tag{7}$$

In this paper, the assumptions are made as follows:

Assumption 1 There is a positive definite matrix $X = \mathrm{diag}\{x_i\}$ $(i = 1, 2, \ldots, n)$ such that the observer gain $L = X\mathcal{C}^*(v^{\mathrm{s}}(t))$ generates a C_0 semigroup, where $s_i > 0$ is the feedback gain.

Assumption 2 The operator $-\mathcal{A}$ is coercive, indicating that there is a positive constant σ such that $\mathrm{Re}\langle -\mathcal{A}\phi, \phi \rangle \geq \sigma \|\phi\|^2$.

Theorem 1 Given the proposed state system (3) consisting of at most n sensor devices, each mobile sensor agent velocity is given by

$$\dot{v}_i^{\mathrm{s}} = -\sigma_i[\zeta^2(t, v_i^{\mathrm{s}} - \varepsilon) - \zeta^2(t, v_i^{\mathrm{s}} + \varepsilon)],$$

where the velocity gain for each sensor agent $\sigma_i > 0, i = 1, 2, \ldots, n$, then the state observer (6) asymptotically converges to the state system (3) and forms a stable error evolution system.

Proof Take the associated Lyapunov functional

$$V(t) = -\langle \zeta(t), \mathcal{A}_{LC}(v^{\mathrm{s}}(t))\zeta(t) \rangle. \tag{8}$$

According to Assumption 1, it is derived that $V(t) \geq 0$. Then the derivative of Eq. (8) along the observation error (7) becomes

$$\begin{aligned} \dot{V}(t) =& -\langle \dot{\zeta}(t), \mathcal{A}_{LC}(v^{\mathrm{s}}(t))\zeta(t) \rangle - \langle \zeta(t), \mathcal{A}_{LC}(v^{\mathrm{s}}(t))\dot{\zeta}(t) \rangle \\ & - \langle \zeta(t), \frac{\mathrm{d}}{\mathrm{d}t}(\mathcal{A}_{LC}(v^{\mathrm{s}}(t)))\zeta(t) \rangle \\ =& -2\langle \mathcal{A}_{LC}(v^{\mathrm{s}}(t))\zeta(t), \mathcal{A}_{LC}(v^{\mathrm{s}}(t))\zeta(t) \rangle \\ & + 2\langle \zeta(t), X\frac{\partial \mathcal{C}(v^{\mathrm{s}}(t))}{\partial t}\mathcal{C}(v^{\mathrm{s}}(t))\zeta(t) \rangle \\ =& -2\|\mathcal{A}_{LC}(v^{\mathrm{s}}(t))\zeta(t)\|^2 + 2\int_0^h \zeta^2(t, v)X\dot{v}^{\mathrm{s}}(t) \\ & \times \frac{\partial}{\partial t}\{c(v, v^{\mathrm{s}}(t))\}c(v, v^{\mathrm{s}}(t))\,\mathrm{d}v \\ =& -2\|\mathcal{A}_{LC}(v^{\mathrm{s}}(t))\zeta(t)\|^2 + 2\sum_{i=1}^{n}\dot{v}_i^{\mathrm{s}}(t)\int_0^h \zeta^2(t, v) \\ & \times x_i[\delta(v_i^{\mathrm{s}} - \varepsilon) - \delta(v_i^{\mathrm{s}} + \varepsilon)]c_i(v, v^{\mathrm{s}}(t))\,\mathrm{d}v \\ =& -2\|\mathcal{A}_{LC}(v^{\mathrm{s}}(t))\zeta(t)\|^2 + 2\sum_{i=1}^{n}\dot{v}_i^{\mathrm{s}}(t)[\zeta^2(t, v_i^{\mathrm{s}} - \varepsilon) \\ & - \zeta^2(t, v_i^{\mathrm{s}} + \varepsilon)]x_i c_i(v, v^{\mathrm{s}}(t)). \end{aligned}$$

Due to $c_i(v, v^{\mathrm{s}}(t)) \geq 0$, if the mobile sensor velocity $\dot{v}_i^{\mathrm{s}} = -\sigma_i[\zeta^2(t, v_i^{\mathrm{s}} - \varepsilon) - \zeta^2(t, v_i^{\mathrm{s}} + \varepsilon)]$ with $\sigma_i > 0$ is selected, we can get $\dot{V}(t) \leq 0$, thus $\lim_{t\to\infty} e(t) = 0$. Then, a stable estimation error system can be guaranteed.

4. Event-triggered control

4.1. Controller design

An event-triggered control loop (Fig. 1) is considered in the present study. With an event generator, the triggering condition is continuously monitored so as to determine whether an event occurs. If an event occurs at instants t_k, $k = 1, 2, \ldots$, the event generator sends the latest estimated state $\bar{s}(t_k)$ to the controller. It is assumed that $t_0 = 0$. In other words, the first event occurs at time t_0. In the successive time interval $t \in [t_k, t_{k+1})$, the controller is only updated at time t_k. Then, the state-feedback controller is determined according to the observer state

$$u(t) = -K\bar{s}(t_k), \quad t \in [t_k, t_{k+1}), \tag{9}$$

where K is the controller feedback gain. The $(k+1)$-th event can be defined as

$$\|e(t)\|^2 \geq \delta\|\bar{s}(t)\|^2, \tag{10}$$

where $e(t) = \bar{s}(t) - \bar{s}(t_k)$, $\delta \in [0, 1)$.

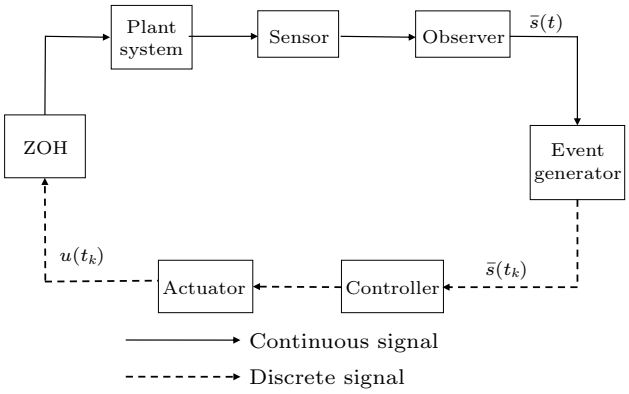


Fig. 1. Event-triggered control system.

4.2. Stability analysis

In the period $t \in [t_k, t_{k+1})$, the plant system (3) under the control input (9) is rewritten as

$$\begin{aligned}\dot{s}(t) =& (\mathcal{A} - \mathcal{B}(v^{\mathrm{a}}(t))K)s(t) - \mathcal{B}(v^{\mathrm{a}}(t))K\zeta(t) \\ &+ \mathcal{B}(v^{\mathrm{a}}(t))Ke(t). \end{aligned} \tag{11}$$

Here, we take $\mathcal{B} = \mathcal{B}(v^{\mathrm{a}}(t))$ and $\mathcal{C} = \mathcal{C}(v^{s}(t))$. Based on the definition $\vartheta(t) = [s(t), \zeta(t)]^{\mathrm{T}}$, from the above plant system (3) and observation error dynamic equation (7), a closed-loop system is determined:

$$\dot{\vartheta}(t) = \bar{\mathcal{A}}\vartheta(t) + \bar{\mathcal{B}}e(t), \tag{12}$$

where

$$\bar{\mathcal{A}} = \begin{bmatrix} \mathcal{A} - \mathcal{B}K & -\mathcal{B}K \\ 0 & \mathcal{A} - L\mathcal{C} \end{bmatrix}, \quad \bar{\mathcal{B}} = \begin{bmatrix} \mathcal{B}K \\ 0 \end{bmatrix}.$$

Theorem 2 The closed-loop system (12) is considered under the triggering condition determined by Eq. (10). For given gains K and L, if there exist a positive definite symmetric matrix $P = P^{\mathrm{T}} > 0$ and a real number $\delta \in [0, 1)$, an inequality holds:

$$Q = \bar{\mathcal{A}}^{\mathrm{T}}P + P\bar{\mathcal{A}} + P\bar{\mathcal{B}}\bar{\mathcal{B}}^{\mathrm{T}}P + \delta I_n < 0. \tag{13}$$

Then the state of the system (12) is globally asymptotically stable.

Proof On the basis of the triggering condition (10), if $t \in [t_k, t_{k+1})$, we can obtain

$$\|e(t)\|^2 < \delta\|\bar{s}(t)\|^2 = \delta\|s(t) - \zeta(t)\|^2 = \delta\vartheta^{\mathrm{T}}(t)I_n\vartheta(t), \tag{14}$$

where $I_n = I_2^{\mathrm{T}}I_2$, $I_2 = [I, I]$.

The Lyapunov function is constructed as follows:

$$V(t) = \vartheta^{\mathrm{T}}(t)P\vartheta(t), \tag{15}$$

where the positive definite symmetric matrix $P = P^{\mathrm{T}} > 0$ is the solution to the inequality (13). The derivative of Eq. (15) along the closed-loop system (12) becomes

$$\begin{aligned}\dot{V}(t) =& [\bar{\mathcal{A}}\vartheta(t) + \bar{\mathcal{B}}e(t)]^{\mathrm{T}}P\vartheta(t) + \vartheta^{\mathrm{T}}(t)P[\bar{\mathcal{A}}\vartheta(t) + \bar{\mathcal{B}}e(t)] \\ =& \vartheta^{\mathrm{T}}(t)(\bar{\mathcal{A}}^{\mathrm{T}}P + P\bar{\mathcal{A}})\vartheta(t) + \mathrm{e}^{\mathrm{T}}(t)\bar{\mathcal{B}}^{\mathrm{T}}P\vartheta(t) \\ &+ \vartheta^{\mathrm{T}}(t)P\bar{\mathcal{B}}e(t) \\ =& \vartheta^{\mathrm{T}}(t)(\bar{\mathcal{A}}^{\mathrm{T}}P + P\bar{\mathcal{A}})\vartheta(t) - \|e(t) - \bar{\mathcal{B}}^{\mathrm{T}}P\vartheta(t)\|^2 \\ &+ \vartheta^{\mathrm{T}}(t)P\bar{\mathcal{B}}\bar{\mathcal{B}}^{\mathrm{T}}P\vartheta(t) + \|e(t)\|^2 \\ \le& \vartheta^{\mathrm{T}}(t)(\bar{\mathcal{A}}^{\mathrm{T}}P + P\bar{\mathcal{A}} + P\bar{\mathcal{B}}\bar{\mathcal{B}}^{\mathrm{T}}P)\vartheta(t) + \|e(t)\|^2 \\ =& \vartheta^{\mathrm{T}}(t)(\bar{\mathcal{A}}^{\mathrm{T}}P + P\bar{\mathcal{A}} + P\bar{\mathcal{B}}\bar{\mathcal{B}}^{\mathrm{T}}P + \delta I_n)\vartheta(t) \\ =& \vartheta^{\mathrm{T}}(t)Q\vartheta(t). \end{aligned}$$

According to the inequality (13), $\dot{V}(t) < 0$. Thus, the system (12) is globally asymptotically stable.

4.3. Zeno behavior analysis

The Zeno behavior generally exists in an event-triggered control system, but the actual control system requires no Zeno behavior. This section shows that a positive minimum inter-event interval always exists, therefore the closed-loop system does not have Zeno behavior.

Theorem 3 The sampling instants determined by the triggering condition (10) indicate that the minimum inter-event interval $T_{\min}$ between two consecutive events has a positive lower bounded.

Proof The observer state is further considered as

$$\begin{aligned}\dot{\bar{s}}(t) &= \mathcal{A}\bar{s}(t) - \mathcal{B}K\bar{s}(t_k) - L(\mathcal{C}\bar{s}(t) - \mathcal{C}s(t)) \\ &= (\mathcal{A} - \mathcal{B}K)\bar{s}(t) + \mathcal{B}Ke(t) - L\mathcal{C}\zeta(t). \end{aligned}$$

Based on the triggering condition, if $\|e(t)\| < \delta\|\bar{s}(t)\|$ holds for all $t \in [t_k, t_{k+1})$, there will be no event generated.

According to the observation error state (7), we get

$$\begin{aligned}\|e(t)\| &< \sqrt{\delta}\|\bar{s}(t)\| \\ &< \sqrt{\delta}\|\zeta(t)\| + \sqrt{\delta}\|s(t)\| \\ &< \sqrt{\delta}(2\|\zeta(t)\| + \bar{s}(t)\|). \end{aligned}$$

Due to $\delta \in [0, 1)$, we can reach

$$-\frac{\|\zeta(t)\|}{|\bar{s}(t)\|} < \frac{1}{2} - \frac{\|e(t)\|}{2\|\bar{s}(t)\|}.$$

The lower bound is calculated with the following dynamics of $\|e(t)\|/\|\bar{s}(t)\|$:

$$\begin{aligned}\frac{\mathrm{d}}{\mathrm{d}t}\frac{\|e(t)\|}{\|\bar{s}(t)\|} &= \frac{\mathrm{e}^{\mathrm{T}}(t)\dot{e}(t)}{\|\bar{s}(t)\|\|e(t)\|} - \frac{\dot{\bar{s}}(t)\|\bar{s}^{\mathrm{T}}(t)\|\|e(t)\|}{\|\bar{s}(t)\|\|\bar{s}^{\mathrm{T}}(t)\|^2} \\ &\le \frac{\dot{\bar{s}}(t)}{\|\bar{s}(t)\|}\Big(1 + \frac{\|e(t)\|}{\|\bar{s}(t)\|}\Big) \\ &\le (\| \mathcal{A} - \mathcal{B}K \| + \|\mathcal{B}K\|\frac{\|e(t)\|}{\|\bar{s}(t)\|} + \frac{1}{2}\| L\mathcal{C} \| \\ &\quad + \frac{1}{2}\| L\mathcal{C} \|\frac{\|e(t)\|}{\|\bar{s}(t)\|})\Big(1 + \frac{\|e(t)\|}{\|\bar{s}(t)\|}\Big) \\ &\le \Big[\Big(\| \mathcal{A} \| + \| \mathcal{B}K \| + \frac{1}{2}\| L\mathcal{C} \| \Big) \end{aligned}$$

$$+\Big(\parallel \mathcal{B}K \parallel +\frac{1}{2}\parallel \mathcal{L}\mathcal{C} \parallel\Big)\frac{\|e(t)\|}{\|\bar{s}(t)\|}\Big]\Big(1+\frac{\|e(t)\|}{\|\bar{s}(t)\|}\Big).$$

If $r(t)=\|e(t)\|/\|\bar{s}(t)\|$, $\omega=\parallel \mathcal{A} \parallel + \parallel \mathcal{B}K \parallel +\frac{1}{2}\parallel \mathcal{L}\mathcal{C} \parallel$, and $\eta=\parallel \mathcal{B}K \parallel +\frac{1}{2}\parallel \mathcal{L}\mathcal{C} \parallel$, then we have the estimate $\dot{r}\le(\omega+\eta r)(1+r)$.

The solution can be obtained with the initial state $r(0)=0$ as follows:

$$r(t)=\frac{\omega-\omega\,\mathrm{e}^{(\eta-\omega)t}}{\omega\,\mathrm{e}^{(\eta-\omega)t}-\eta}.$$

According to condition (10), we get $r(\tau)=\sqrt{\delta}(\delta\neq 0)$ at the occurrence time of an event. Then, the minimum inter-event interval is calculated as

$$\tau=\frac{1}{\eta-\omega}\ln\frac{\eta\sqrt{\delta}+\omega}{\omega(1+\sqrt{\delta})}.$$

Since $\omega=\parallel \mathcal{A} \parallel + \parallel \mathcal{B}K \parallel +\frac{1}{2}\parallel \mathcal{L}\mathcal{C} \parallel>0$, $\eta=\parallel \mathcal{B}K \parallel +\frac{1}{2}\parallel \mathcal{L}\mathcal{C} \parallel>0$, and $n>m, 0\le\delta<1$, then we get $\ln\frac{\eta\sqrt{\delta}+\omega}{n(1+\sqrt{\delta})}<0$, thus, $\tau=\frac{1}{\eta-\omega}\ln\frac{\eta\sqrt{\delta}+\omega}{\omega(1+\sqrt{\delta})}>0$, which gives a positive lower bounded on the time $T_{\min}$ ($T_{\min}\ge\tau$). In other words, the Zeno behavior can be excluded.

5. Guidance of mobile actuator agents

For each time interval defined by the event-triggered control (9), an actuator guidance algorithm determining the optimal moving displacement of the actuator is developed. A single actuator is assumed to be able to move at a predetermined position within the spatial domain. Under this assumption, the control signal updates the newest state estimates at event time t_k and the actuator changes the displacement at the beginning of each time interval $[t_k,t_{k+1})$. To address the issue stated above, the following optimal actuator moving algorithm is proposed.

Algorithm 1 (1) Through the event-triggered control for state observer, a series of unequal time intervals $[t_k,t_{k+1})$ can be obtained as the displacement switching time of the actuator, where $k=1,2,\ldots$.

(2) At each t_k, the cost functional is considered as

$$J_k=\int_0^{\infty}\langle y(\tau),y(\tau)\rangle+\langle u(\tau),Ru(\tau)\rangle\,\mathrm{d}\tau,$$

where R is a coercive bounded operator. According to the linear quadratic optimal regulator, its optimal value is

$$J^{\mathrm{opt}}=\langle s(t_k),\Pi_p(t_k)s(t_k)\rangle,$$

where $\Pi_p(t)$ is the solution of the operator Riccati equation

$$\begin{aligned}&\langle(\mathcal{A}-\mathcal{B}K)\varphi_1,\Pi_p(t)\varphi_2\rangle+\langle\Pi_p(t)\varphi_1,(\mathcal{A}-\mathcal{B}K)\varphi_2\rangle\\&=-\langle\mathcal{C}\varphi_1,\mathcal{C}\varphi_2\rangle\end{aligned}$$

for $\varphi_1,\varphi_2\in D(\mathcal{A})$.

(3) At the beginning of each time subinterval $[t_k,t_{k+1})$, the minimum value of the quadratic optimal indices corresponding to mobile actuator position is chosen as

$$v^{\mathrm{a}}(t_k)=\arg\min_{v^{\mathrm{a}}\in\Omega}\langle s(t_k),\Pi_p(t_k)s(t_k)\rangle.$$

(4) Steps 2 and 3 are performed again for the new subinterval $[t_{k+1},t_{k+2})$.

Remark 1 If the actuator moves within a limited range at each time, which means that the actuator can move from the current position $v^{\mathrm{a}}(t_k)$ to the domain $[v^{\mathrm{a}}(t_k)-h,v^{\mathrm{a}}(t_k)+h]$. In this way, the actuator position is readjusted as

$$v^{\mathrm{a}}(t_k)=\arg\min_{v^{\mathrm{a}}(t_{k-1})-h\le v^{\mathrm{a}}\le v^{\mathrm{a}}(t_{k-1})+h}\langle s(t_k),\Pi_p(t_k)s(t_k)\rangle.$$

Remark 2 From the results of linear operator inequalities for infinite dimensional systems, it can be easily conclude that the feedback controller $u(t)=-K\bar{s}(t_k)$ is a stabilizing one regardless of the actuators used. Equivalently, the closed-loop operator $\mathcal{A}-\mathcal{B}(v_i^{\mathrm{a}}(t))K$ generates an exponentially stable C_0 semigroup for all actuators $v_i^{\mathrm{a}}(t), i=1,\ldots,m$. That is, the mobile actuators do not affect the closed-loop system stability.

6. Numerical results

A reaction-diffusion equation described by DPS (1) and (2) with $\alpha(v)=0.008$ in $[0,h]=[0,1]$ is considered. The initial value is $s(0,v)=\cos(\pi v)\,\mathrm{e}^{-7v^2}$. The observer gain and initial condition are expressed as $L=XC^*$ with $X=\mathrm{diag}\{3,3,3,3\}$ and $\bar{s}(0,v)=2\sin(\pi v)\,\mathrm{e}^{-7v^2}$. The closed-loop system is simulated in the time interval $[0,50]$ s with $m=4$ mobile sensors and $n=1$ mobile actuator, where the initial locations of sensors and actuators are set as $v_1^{\mathrm{s}}=0.1$, $v_2^{\mathrm{s}}=0.4$, $v_3^{\mathrm{s}}=0.6$, $v_4^{\mathrm{s}}=0.9$, and $v_1^{\mathrm{a}}=0.55$. The controller gain $K=2$ and sensor velocity gains $\sigma_1=\sigma_2=\sigma_3=\sigma_4=1$.

Figure 2 shows the trajectories of the sensor agents for mobile (solid lines) and fixed (dotted lines) cases. Based on the proposed stable guidance scheme, it can be seen that the mobile sensors move to the center of the spatial domain.

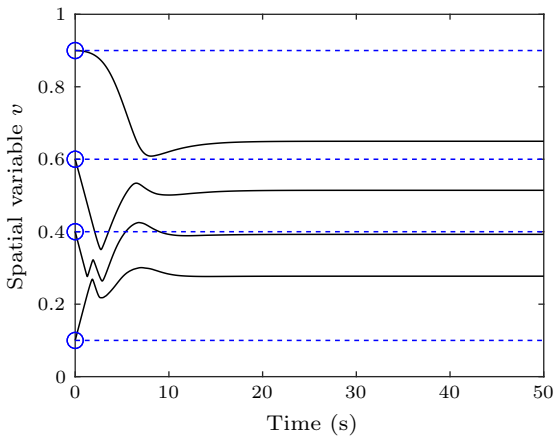


Fig. 2. Sensor trajectories.

Taking $\delta = 0.81$ in the event-triggered condition (10), the dynamic behavior of the event-triggered control is presented in Fig. 3. After the first event at time $t_0 = 0$, the subsequent events are triggered respectively at $t_1 = 3.8$ s, $t_2 = 8.633$ s, $t_3 = 14.77$ s, $t_4 = 22.13$ s, $t_5 = 29.23$ s, $t_6 = 35.57$ s, $t_7 = 42.1$ s and $t_8 = 49.4$ s in $[0, 50]$ s. In the event-triggered time interval $[t_k, t_{k+1})$, the optimal mobile actuator switching trajectories are depicted in Fig. 4.

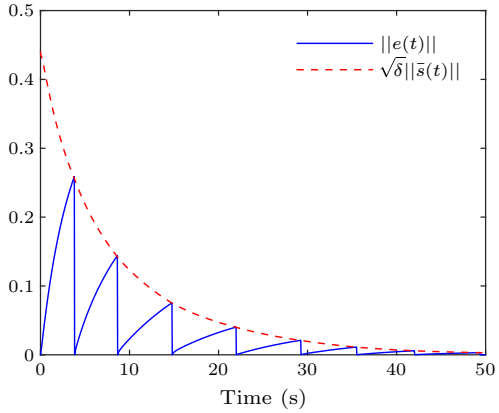


Fig. 3. Simulation result with the event-triggered mechanism.

The evolution comparison of the closed-loop system L_2 state norms for four cases is depicted in Fig. 5, case 1 (a fixed actuator based on time-triggered), case 2 (a mobile actuator based on event-triggered with a fixed threshold, where $e_0 = 0.05$), case 4 (proposed in this paper) are all placed in the same initial position. When the event-triggered control with a dynamic threshold is implemented, the state norm converges to zero faster than that in other methods.

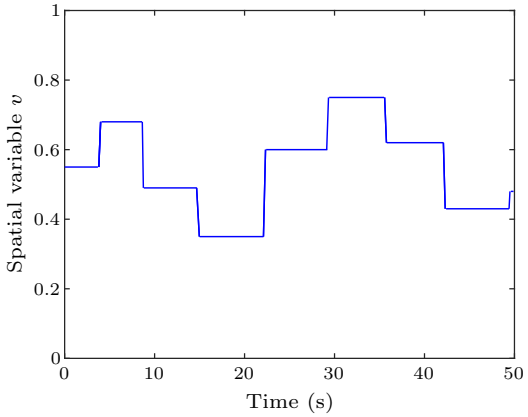


Fig. 4. The optimal actuator trajectory.

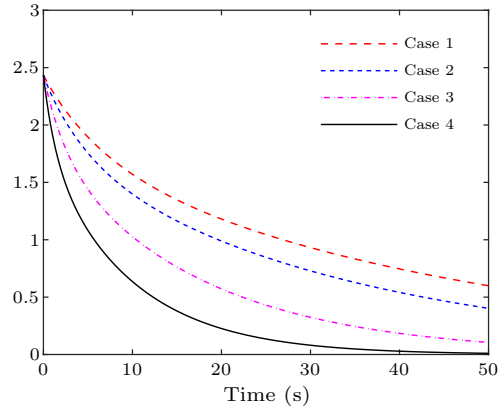


Fig. 5. Evolution of closed-loop system norm for four different cases.

The cumulative norms for the four cases are tabulated in Table 1, once again, as can be observed by comparison, the scheme developed in this paper shows enhanced performance.

Table 1. L_2 state norm.

Case	Time (s)	Norm
Time-triggered-fixed actuator	5	3.1089
Time-triggered-fixed actuator	20	10.4363
Time-triggered-fixed actuator	50	19.7795
Time-triggered-mobile actuator	5	3.0091
Time-triggered-mobile actuator	20	9.5527
Time-triggered-mobile actuator	50	17.3922
Event-triggered-mobile actuator-fixed threshold	5	2.7289
Event-triggered-mobile actuator-fixed threshold	20	7.7321
Event-triggered-mobile actuator-fixed threshold	50	12.9705
Event-triggered-mobile actuator-time-varying threshold	5	2.3767
Event-triggered-mobile actuator-time-varying threshold	20	5.9604
Event-triggered-mobile actuator-time-varying threshold	50	9.6369

7. Conclusion

An event-triggered control scheme of DPSs with mobile sensors and actuators is addressed. The scheme is based on a state feedback observer which is designed according to the measurement information obtained with the mobile sensors. The mobile actuator does not update its displacement until the error signal exceeds a dynamic threshold. Furthermore, the stability of the closed-loop system and nonzero minimum inter-event interval can be established. The comparison with other methods illustrates that the the presented control scheme is less conservative.

Acknowledgment

Project supported by the National Natural Science Foundation of China (Grant No. 62073045).

References

[1] Kuto K, Matsuzawa H and Peng R 2017 *Calc. Var. Partial. Dif.* **56** 112
[2] Ren X, Yu M, Zhao X, Li J, Zheng S M, Chen F C Wang Z Y, Zhou J Y, Pei G and Ji J 2020 *Energy* **190** 116338
[3] Guo D, Xu M and Chen S L 2013 *Acta Aerodynamica Sinica* **31** 413 (in Chinese)
[4] My C A and Bien D X 2020 *Int. J. Adv. Robot. Syst.* **17** 1
[5] El-Farra N H, Demetriou M A and Christofides P D 2008 *Chem. Eng. Sci.* **63** 3537
[6] Iftime O V and Demetriou M A 2009 *Automatica* **45** 312
[7] Demetriou M A 2010 *IEEE Trans. Automat. Control* **55** 1570
[8] Ji H H, Cui B T and Liu X Z 2011 *Commun. Nonlinear Sci.* **98** 105773
[9] Ji H H and Cui B T 2022 *Fuzzy Set. Syst.* **432** 28
[10] Bhave G, Chen J C, Singer A, Sharma A and Robinson J T 2021 *Mater. Today* **46** 125
[11] Chen C H, Lin M Y, Shih Y C and Chen C C 2022 *Microprocessors Microsytems* **99** 104507
[12] Demetriou M A 2010 *IEEE Trans. Automat. Control* **55** 1570
[13] Demetriou M A 2012 *IEEE Trans. Automat. Control* **57** 2979
[14] Jiang Z X, Cui B T and Lou X Y 2014 *IFAC Proc.* **47** 6490
[15] Zhang J Z, Cui B T and Bo Z 2017 *Chin. Phys. B* **26** 090201
[16] Zhang J, Cui B, Dai X and Jiang Z 2020 *IEEE/CAA J. Automat. Sin.* **7** 865
[17] Fu H S, Cui B T, Zhuang B and Zhang J Z 2021 *Mathematics* **9** 1
[18] Xiao X Q, Ju H P, Zhou L and Lu G P 2019 *Automatica* **111** 108585
[19] Qian Y Y and Wan Y 2021 *Automatica* **133** 109837
[20] Hu S, Qiu J, Chen X, Zhao F and Jiang X 2022 *IET Control Theory A* **16** 475
[21] Li X N, Wu H Q and Cao J D 2023 *Math. Comput. Simulat.* **203** 647
[22] Jiang Z X, Cui B T, Wu W and Zhuang B 2016 *Comput. Math. Appl.* **72** 2854
[23] Ji H H, Zhang H and Cui B T 2018 *J. Franklin Institute* **355** 5928
[24] Song X N, Wang M, Song S and Lu J W 2020 *J. Franklin Institute* **357** 11368
[25] Mu W Y, Qiu F, Zhuang B and Chen L G 2021 *J. Franklin Institute* **358** 384